

Improved Simulation of Image Detail Visibility using the Non-Subsampled Contourlet Transform

Marius Pedersen, Xinwei Liu, and Ivar Farup.

The Norwegian Colour and Visual Computing Laboratory, Gjøvik University College (Norway).

Abstract

A previous study proposed a method for simulation of detail visibility of natural images (from different observation distances) by using contrast sensitivity functions and wavelets (Pedersen and Farup, Color and Imaging Conference 2012). In this paper we propose an improved method using the non-subsampled contourlet transform, which accounts for important aspects of the human visual system such as orientation sensitivity. In addition we account for the effect of surround illumination. Objective and subjective evaluations show that the proposed methodology is promising, and that it introduces fewer artifacts than the previous method.

Introduction

Pedersen and Farup [1] presented at the 20th Color and Imaging Conference a method for simulating image detail visibility of natural images, where perceptible information at a given distance is kept, while imperceptible information is discarded. If the original and the simulated image are viewed from the simulated distance or farther away, they should be indistinguishable. This is because the information from the original, that is imperceptible, has been removed through the simulation. Such a method to simulate detail visibility has several applications; it can be used in the evaluation of image quality, improve compression, gamut mapping, and halftoning. The method is based on the relationship between contrast sensitivity and spatial frequency (contrast sensitivity functions), and an octave-wise spread over the spatial frequency range matched by wavelet decompositions. The method showed promising results; giving a good match to human observers and improving the performance of an image quality metric. The method had several advantageous properties, such as multi-resolution from coarse to fine resolutions and the basis elements in the representation are localized in both spatial and the frequency domains.

However, since it uses wavelets it suffers from artifacts, such as blocking and ringing. These artifacts are unwanted, and if they are suprathreshold they become visible for observers. Wavelets have a crude directional representation (primarily vertical, horizontal, and diagonal). Although they are good at representing point discontinuities, they are not good at representing discontinuities along edges. Therefore, the representation should contain basis elements oriented in a variety of directions, preferably in more directions than those offered by wavelets. Additionally, wavelets are isotropic, and they are therefore not able to capture smooth contours in images, which often occurs in natural

images. Hence, the representation should contain basis elements using a variety of elongated shapes with different aspect ratios, which can be accomplished with for example curvelets [2] or contourlets [3]. Furthermore, the model by Pedersen and Farup [1] does not incorporate a model of the Contrast Sensitivity Function (CSF) that accounts for the fact that we are less sensitive oblique angles than vertical and horizontal angles [4, 5].

In this work we extend the method proposed by Pedersen and Farup [1] by increasing the directionality and better capture smooth contours through the use of the Non-Subsampled Contourlet Transform (NSCT) [6]. Additionally, we incorporate a more advanced CSF model from Barten [7]. All with the goal of improving the simulation of image detail visibility of natural images.

This paper is organized as follows: first we introduce relevant background, then we present the proposed methodology. Further, evaluation of the proposed method is presented. At last we conclude and propose future work.

Background

The method proposed by Pedersen and Farup [1] was based on several different works [8–11]. The image to be filtered was first converted into a suitable color space. For this a linear RGB color space inspired by the $Y\bar{C}_b\bar{C}_r$ color space was used, where the primaries were defined according to the wavelengths of the monochromatic light sources used to generate the gratings used in the experiments by Mullen [12] to measure the chromatic CSFs. Further, the filtering method was based on existing work on local band-limited contrast for complex images [8] and wavelet based contrast sensitivity filtering [9]. A wavelet decomposition of the image was carried out to obtain octave width bands of frequencies. The coefficients were reconstructed to full-scale before CSFs are applied. The CSF filtered coefficients were compared to the contrast low-pass band, if the filtered coefficients were higher than the low-pass coefficients, the information was kept, else it was removed. Additionally, contrast masking was incorporated using an extended intra channel masking method accounting for local activity [13]. For more information we refer the reader to Pedersen and Farup [1].

The non-subsampled contourlet transform

The NSCT was proposed by da Cunha et al. [6], and it was based on a non-subsampled pyramid structure and non-subsampled directional filter banks. The design results in a flexible multi-scale, multi-direction, and shift in-

variant image decomposition. The NSCT can be divided into two shift-invariant parts: a non-subsampled pyramid structure to achieve multi-scale properties and a non-subsampled filter bank with directional filters. The first part gave a sub-band decomposition similar to that of the Laplacian pyramid, which was done through the usage of two-channel non-subsampled 2-D filter banks. For the latter, a directional filter was constructed by combining critically-sampled two-channel fan filter banks and re-sampling operations. This results in a tree-structured filter bank that splits the 2-D frequency plane into directional wedges. These two elements were combined as seen in Figure 1.

The NSCT has shown to be effective for image quality assessment [14], image fusion [15], face recognition [16], denoising [6, 17, 18], and enhancement [6, 19]. It is therefore likely, together with its advantageous properties, that it will be effective also for the simulation of image detail visibility.

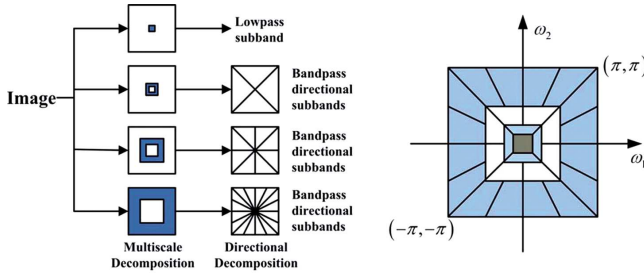


Figure 1. Non-Subsampled Contourlet Transform (NSCT). On the left the non-subsampled filter bank structure and on the right the idealized frequency partitioning obtained by the non-subsampled filter bank. Figure reproduced from Lu et al. [14].

Proposed methodology

The input image is transformed into the Ybr color space as proposed by Pedersen and Farup [1]. Then each channel is decomposed using the NSCT. Unless stated otherwise we decompose the image using three levels with 4, 8, and 16 orientations, where the pyramidal filter generated from a 1-D filter using a maximally flat mapping function with 4 vanishing moments, and the directional filter is a 2-D diamond maxflat filter of order 7. These are the default filters proposed by da Cunha et al. [6]. This gives us a low-pass filtered version (LL) and high-pass filtered versions h_ψ in several orientations ψ . The high-pass filtered coefficients are filtered with CSFs. For the achromatic channel (Y) a luminance CSF is applied, and for the two chromatic channels (b and r) chromatic CSFs are applied. Due to the division into orientations using the non-subsampled contourlet, the CSF needs to be adapted to the orientation. We apply the CSF model from Barten [7] that incorporate orientation dependence of the CSF and the effect of surround illumination. The general formula for the luminance CSF is

$$CSF_L(u) = \frac{C \exp(-0.0016u^2(1+100/L)^{0.08})}{\sqrt{\left(1 + \frac{144}{X_0^2} + 0.64u^2\right)\left(\frac{63}{L^{0.83}} + \frac{1}{1-\exp^{-0.02u^2}}\right)}}, \quad (1)$$

where C is a constant adapted to CSF measurements. Barten [7] reports values from 3700 to 5800 for C depending on the measurements. Unless stated otherwise a value of 3700 has

been used. u is the spatial frequency in cycles per degree, L is the luminance in cd/m^2 , and X_0^2 is the angular object area in square degrees. In order to account for the fact that contrast sensitivity decreases for oblique gratings, a continuous function of the orientation angle is added to the CSF formula in Equation 1, following the recommendation by Barten [7]:

$$CSF_L(u) =$$

$$\frac{C \exp\left(-0.0016u^2(1+100/L)^{0.08}\right)}{\sqrt{\left(1 + \frac{144}{X_0^2} + 0.64(1+3\sin^2(2\varphi)u^2)\left(\frac{63}{L^{0.83}} + \frac{1}{1-\exp^{-0.02u^2}}\right)\right)}}, \quad (2)$$

where φ is the orientation angle in degrees.

Further, the visibility of an object, and thus the contrast sensitivity, can be reduced if the object is surround by a dark surround, and also in the opposite situation. This can be included in the CSF formula with a simple multiplicative correction factor, f , as proposed by Barten [7]:

$$f = \exp\left(-\frac{\ln^2\left(\frac{L_s}{L}\left(1 + \frac{144}{X_0^2}\right)^{0.25}\right) - \ln^2\left(\left(1 + \frac{144}{X_0^2}\right)^{0.25}\right)}{2\ln^2(32)}\right), \quad (3)$$

where L is the luminance of the object, L_s is the surround luminance, and X_0^2 is the object area in square degrees of visual angle.

For the chromatic content, two CSFs are required, one for the red-green channel and one for the blue-yellow channel. For these channels we apply the CSFs from Johnson and Fairchild [20]:

$$CSF_C = \alpha_1 \exp(-\beta_1 u^{\gamma_1}) + \alpha_2 \exp(-\beta_2 u^{\gamma_2}), \quad (4)$$

where the parameters for the red-green and blue-yellow channels are given by Table 1, and u is defined as cycles per degree.

Table 1: Parameters for the chrominance CSFs.

| Parameter | red-green channel | blue-yellow channel |
|------------|-------------------|---------------------|
| α_1 | 109.14130 | 7.032845 |
| β_1 | -0.00038 | -0.000004 |
| γ_1 | 3.42436 | 4.258205 |
| α_2 | 93.59711 | 40.690950 |
| β_2 | -0.00367 | -0.103909 |
| γ_2 | 2.16771 | 1.648658 |

The luminance CSF (CSF_L) is applied to the luminance channel (Y), and the chrominance CSFs (CSF_C) are applied to the chrominance channels (b and r) for each band and orientation. It should be noted that the CSF functions are not normalized and applied directly at the given scale.

Now, let $l'_j(x, y)$ denote the contrast filtered LL band and $h_{\psi j}(x, y)$ denote the high pass bands bands (depending on the orientation ψ) at level j . At the lowest level, the LL band is not filtered, thus $l'_N(x, y) = l_N(x, y)$, where N denotes the lowest level. Further, let $a_{\psi j}(x, y)$ denote the CSF

filtered version of $h_{\psi j}(x, y)$ as described above. Then, the contrast filtered octave bands are defined as

$$h'_{\psi j}(x, y) = \begin{cases} h_{\psi j}(x, y) & \text{if } a_{\psi j}(x, y) > l'_j(x, y) \\ 0 & \text{else} \end{cases} \quad (5)$$

The filtered information in ψ orientations are then used to reconstruct the image in order to obtain the low-pass filtered version for the next level.

In addition to filter the image using the CSF, we also incorporate contrast masking as done by Pedersen and Farup [1]. This is accomplished by applying the extended intra channel masking model accounting for local activity as described by Nadenau [13]:

$$a_{\psi j}^M(x, y) = \frac{a_{\psi j}(x, y)}{T_{j, \psi}(x, y)} \quad (6)$$

where $a_{\psi j}^M(x, y)$ is the masked contrast and

$$T_{j, \psi}(x, y) = \max(1, \tilde{c}_{j, \psi}(x, y)^\epsilon) \cdot (1 + \omega_\rho), \quad (7)$$

where T is the threshold elevation, $\tilde{c}_{j, \psi}(x, y)$ is the wavelet coefficients normalized by the CSF for a given level j and orientation ψ at pixel location (x, y) , ϵ is the slope-parameter, and ω_ρ is the correction term for the influence of an active or homogeneous neighborhood:

$$\omega_\rho = \frac{1}{(k_L)^\vartheta N_\rho} \sum_\rho |\tilde{c}_{j, \psi}|^\vartheta, \quad (8)$$

where k_L determines the dynamic range of ω_ρ , N_ρ specifies the number of coefficients in the neighborhood ρ (here an n-by-n neighborhood is used), and ϑ is the power. We have followed the recommendation by Nadenau et al. [21] regarding the parameters ($N_\rho = 84$, $k_L = 3e - 06$, and $\epsilon = 0$, with a 3×3 neighborhood). ϑ is a free parameter, our preliminary testing has shown a value of 0.28 to produce good results. Masking is performed within each color channel and between orientations.

Evaluation of the proposed method

If the original and the simulated image are viewed from the simulated distance or farther away, they should be indistinguishable. This is because the information from the original is imperceptible, and the same information has been removed by the simulation. However, if the original and the simulation are viewed from a distance closer than the simulated distance, the difference in content between the original and the simulation should be visible. Nevertheless, it is still important that information, such as artifacts, is not added to the simulated image. In the worst case artifacts can result in the simulated image becoming distinguishable from the original at the simulated distance or farther away. Artifacts can also reduce the quality of the simulated image when viewed at a distance closer than the simulated distance. Therefore, it is important to avoid artifacts, being the first evaluation criterion.

Visual investigation

One of the drawbacks of the previous filtering method using wavelets [1] was artifacts. We will then therefore compare the new method to the old method, to visually investigate if artifacts like ringing has been reduced. A simple test target with four color patches has been designed to investigate if the new method has less artifacts. The target has been filtered with the new and the old method (Figure 2), and we can clearly see that the proposed method has less prominent ringing, while preserving the edges quite well.

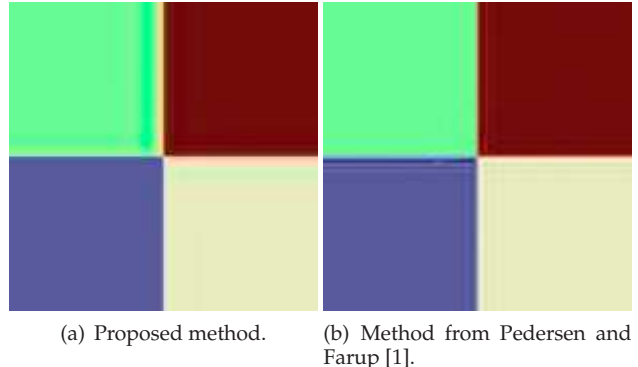


Figure 2. Filtered test target for the evaluation of artifacts (simulated 2 meter). The image has been enlarged to show the artifacts. We can see that the proposed method has fewer artifacts around the edges than the method from Pedersen and Farup [1].

Figure 3 shows an example from a filtered natural image (simulated 2 meters). The proposed method smooths inside regions and has a less noisy appearance compared to the other method. It also has less artifacts around hard edges.



Figure 3. On the left the proposed method and on the right the method from Pedersen and Farup [1]. Both have been simulated for a viewing distance of 2 meters.

Objective evaluation

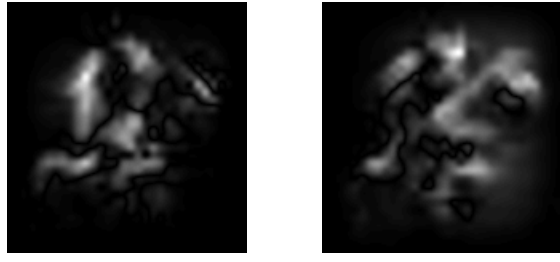
The simulated images should convey the same information as the original image, i.e. it should have the perceptual quality which captures the attention of the observer, also commonly known as saliency. It is important that the simulated images maintain saliency when the simulation method is applied to different areas, such as to improve the quality of gamut mapped or halftoned images.

In this objective evaluation we are using difference of saliency to evaluate if important salient features have been

removed or introduced to the images. Both are unwanted and will reduce the quality if the images. A similar method has been shown to produce good results for evaluation of gamut mapping algorithms [22, 23]. The saliency of the original non-filtered image (Figure 4) and the saliency of the filtered image have been calculated using the graph-based visual saliency model from Harel et al. [24]. This saliency model has shown to correlate well with human perception through eye tracking experiments [25]. The model has been calculated using color, intensity, orientation, and contrast channels. Contrast width is set to 0.05, motion and Gabor angles are set to 0, 45, 90, and 135, otherwise default parameters have been used. Further, we calculate the absolute difference between the saliency of the original image and the saliency of the simulated image. Figure 5 shows the saliency difference for the proposed method (Figure 5(a)) and the previous method [1] (Figure 5(b)). We can see that the proposed method has a lower difference of saliency, indicating that the proposed method maintains saliency better than the old method. Looking at the mean saliency difference, the proposed method has about 30% less difference for the given test image, indicating a better saliency match with the original.



Figure 4. Original image used for evaluation of difference of saliency.



(a) Proposed method. (b) Method from Pedersen and Farup [1].

Figure 5. Difference of saliency between the original image and filtered image (simulated 4 meters). Both are shown the same scale, where black is no loss of saliency and white is maximum loss of saliency. We can clearly see that the proposed method has saliency closer to the original than the old method [1].

Subjective experiment

The proposed method should correspond with visual observations. Therefore, an experiment was conducted, where the original image and the filtered image were presented to observers from a certain distance. If the method is valid, the filtered image and the original should be indistinguishable from a distance equal to or farther than the dis-

tance assumed in the filtered image [26]. The images should be progressively easier to distinguish when the distance becomes shorter than the simulated distance. We will compare the proposed method in this paper to the previously proposed method [1] and the adaptive bilateral filter from Wang and Hardeberg [27, 28]. The latter method avoids undesirable loss of edge information as introduced by a standard CSF-based filtering.

Experimental setup

A total of 14 observers participated in the experiment. All passed a visual acuity test. The observers were shown two images at the time, one original and one filtered image. Their task was to indicate which of the two images that appeared blurred. The images were shown on a Dell 2407WFPb monitor, calibrated to sRGB. The monitor luminance was set to 80 cd/m², according to the sRGB specification. The surround illumination (D50) was set to approximately 30 lux. Three different scenes were used (Figure 6), having red-green, blue-yellow, and achromatic areas. For each of the images two distances were simulated, four and two meters, as in Pedersen and Farup [1].



(a) Image 1: Rock (b) Image 2: Bird (c) Image 3: Cam

Figure 6. Test images used in the evaluation of the proposed method.

The observers started to view the images at a distance larger than the simulated distance, where each image at each simulation distance was presented two times at each viewing distance. The observers indicated which of the two images were blurred. Then the observers moved closer to the monitor, repeating the process. If the observers could not discriminate between the images, they were allowed to guess or skip to the next image (skipping counting as not being able to discriminate the images).

Data analysis

From each distance the percentage of correct identifications of the simulated image was calculated. The distance at which the subjects obtained a 75% identification rate was compared with the simulated distance, as done by Peli [26] and Pedersen and Farup [1]. The measured and simulated distance should be equal if the proposed method corresponds with perception. 95% confidence intervals for the identificate rates have been calculated as Wilson score interval with continuity correction [29].

Visual Experiment Results

Figures 7 and 8 show the results for the three methods (ABF, Pedersen and Farup [1], and the proposed method) when simulating 4 and 2 meters, respectively. For the 4 meter simulation the proposed method shows 65% correct dis-

crimination at 4 meters and 77% at 3.5 meters, indicating that slightly more information could have been removed from the images. However, in a setting where the method is used for optimization of quality (for example image compression) it is preferable that the method filters less rather more information in order to avoid visible artifacts. Additionally, the proposed method shows a favorable linear behavior with a steeper slope compared to the old method [1], while ABF discriminates too much.

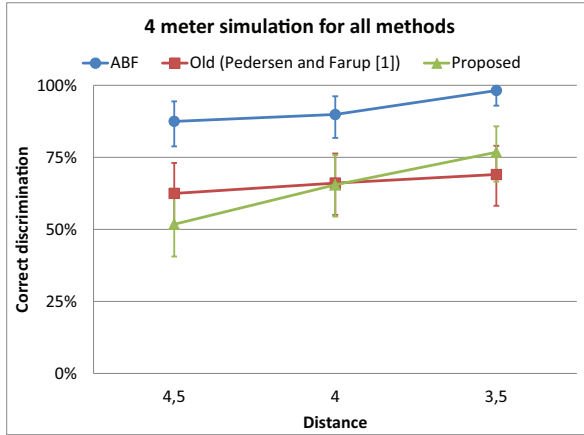


Figure 7. Comparison for the three methods simulating a distance of 4 meters. Discrimination rates are plotted with 95% confidence intervals.

For the 2 meter simulation the proposed method has 76% discrimination at 2 meters, corresponding very well with perception and being more precise than the old method [1]. For the ABF observers fully discriminate for all distances, indicating that ABF is not correlated with the perception of image details. For the proposed method we do not see the same linear behavior as for the 4 meter simulation (Figure 7), it was expected to have a steeper slope between 2 and 1.5 meters. However, the proposed matches the results from the observers well.

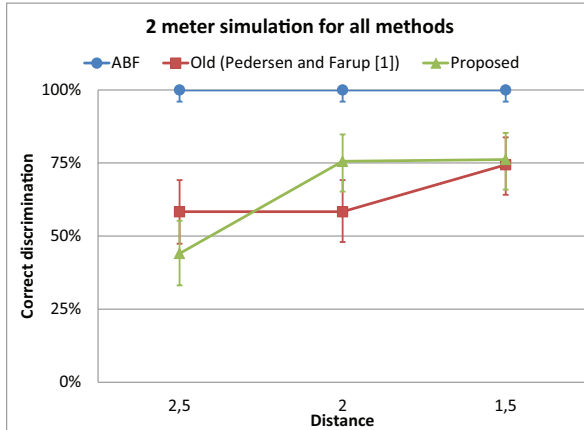


Figure 8. Comparison for the three methods when simulating a distance of 2 meters. Discrimination rates are plotted with 95% confidence intervals.

We have also investigated the results for the individual images when simulating 4 meters (Figure 9) and 2 meters (Figure 10). The proposed method shows similar behavior

for the different images when simulating 4 meters (Figure 9), indicating that the method is producing stable results independent of image content, which is an improvement over the old method. However, there are some differences between the test images; the Rock image (Figure 6(a)) has 76% discrimination at 3.5 meters, corresponding well with observers, while the Cam image (Figure 6(c)) has the lowest discrimination with 63%. For 2 meters (Figure 10) we can still see a similar behavior between the images, except for the Bird image (Figure 6(b)) where the discrimination is reduced at 1.5 meters. This is also the main reason why the slope between 2 and 1.5 meters for all images is not as steep as for 4 meters. Overall, the proposed method is more stable and image independent than the old method [1], where larger individual differences are found between images.

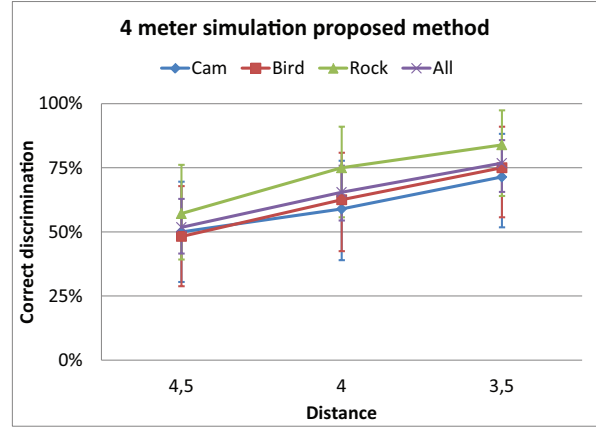


Figure 9. Results for individual images and all images when simulating a distance of 4 meters. Discrimination rates are plotted with 95% confidence intervals.

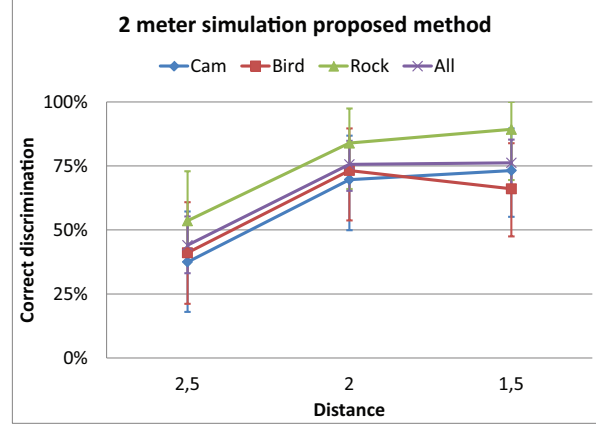


Figure 10. Results for individual images and all images when simulating a distance of 2 meters. Discrimination rates are plotted with 95% confidence intervals.

Conclusion

We have proposed an improved method for simulation of image detail visibility based on the work by Pedersen and Farup [1]. It has been extended through the use of the non-subsampled contourlet transform, that accounts for important aspects of the human visual system such as orientation sensitivity. Additionally, an advanced contrast sensitivity function has been used to account for the effect

of surround illumination. The experimental results from the improved method is very promising, and the simulated images has fewer artifacts than the method from Pedersen and Farup [1].

References

- [1] M. Pedersen and I. Farup. Simulation of image detail visibility using contrast sensitivity functions and wavelets. In *Color and Imaging Conference*, pages 70–75, Los Angeles, CA, November 2012.
- [2] E. J. Candes and D. L. Donoho. Curvelets a surprisingly effective nonadaptive representation for objects with edges. In A. Cohen C. Rabut and L.L. Schumaker., editors, *Curves and Surfaces*. Nashville, TN, Vanderbilt University Press, 2000.
- [3] M.N. Do and M. Vetterli. The contourlet transform: an efficient directional multiresolution image representation. *IEEE Transactions on Image Processing*, 14(12):2091 –2106, dec. 2005.
- [4] F. W. Campbell and J. J. Kulikowski. Orientational selectivity of the human visual system. *J. Physiol.*, 187: 437–445, 1966.
- [5] C. S. Furmanski and S. A. Engel. An oblique effect in human primary visual cortex. *Nat Neurosci*, 3(6):535–536, June 2000. ISSN 1097-6256.
- [6] A. L. da Cunha, J. Zhou, and M. N. Do. The nonsubsampled contourlet transform: Theory, design, and applications. *IEEE Transactions on Image Processing*, 15 (10):3089–3101, Oct. 2006.
- [7] P. G. J. Barten. Formula for the contrast sensitivity of the human eye. In Y. Miyake and D. R. Rasmussen, editors, *Society of Photo-Optical Instrumentation Engineers (SPIE) Conference Series*, volume 5294, pages 231–238, December 2003.
- [8] E. Peli. Contrast in complex images. *J. Opt. Soc. Am. A*, 7:2032–2040, 1990.
- [9] M.J. Nadenau, J. Reichel, and M. Kunt. Wavelet-based color image compression: exploiting the contrast sensitivity function. *IEEE Transactions on Image Processing*, 12(1):58–70, jan 2003.
- [10] M. J. Nadenau and J. Reichel. Opponent color, human vision and wavelets for image compression. In *Color Imaging Conference*, pages 237–242, Scottsdale, AZ, Nov 1999.
- [11] M. Pedersen, G. Simone, M. Gong, and I. Farup. A total variation based color image quality metric with perceptual contrast filtering. In *International conference on Pervasive Computing, Signal Processing and Applications*, Gjøvik, Norway, Sep 2011.
- [12] K. T. Mullen. The contrast sensitivity of human colour vision to red-green and blue-yellow chromatic gratings. *The Journal of Physiology*, 359:381–400, 1985.
- [13] M. Nadenau. *Integration of human color vision models into high quality image compression*. PhD thesis, École Polytechnique Fédérale de Lausanne, 2000.
- [14] F. Lu, Q. Zhao, and G. Yang. Nonsubsampled contourlet transform-based algorithm for no-reference image quality assessment. *Optical Engineering*, 50(6): 067010–067010–10, 2011.
- [15] Q. Zhang and B. I. Guo. Multifocus image fusion using the nonsubsampled contourlet transform. *Signal Processing*, 89(7):1334 – 1346, 2009. ISSN 0165-1684.
- [16] Y. Cheng, Y. Hou, C. Zhao, Z. Li, Y. Hu, and C. Wang. Robust face recognition based on illumination invariant in nonsubsampled contourlet transform domain. *Neurocomputing*, 73(10–12):2217 – 2224, Jun. 2010. ISSN 0925-2312.
- [17] A.L. da Cunha, J. Zhou, and M.N. Do. Nonsubsampled contourlet transform: filter design and applications in denoising. In *IEEE International Conference on Image Processing (ICIP)*, pages 749–52, sep. 2005.
- [18] L. I. Huang, H. z. Wang, and B. Zhu. Adaptive thresholds algorithm of image denoising based on nonsubsampled contourlet transform. In *International Conference on Computer Science and Software Engineering*, volume 6, pages 209 –212, dec. 2008.
- [19] J. Zhou, A.L. Cunha, and M.N. Do. Nonsubsampled contourlet transform: construction and application in enhancement. In *IEEE International Conference on Image Processing (ICIP)*, pages I – 469–72, sep. 2005.
- [20] G. M. Johnson and M. D. Fairchild. Darwinism of color image difference models. In *Color Imaging Conference*, pages 108–112, Scottsdale, AZ, Nov 2001.
- [21] M. J. Nadenau, J. Reichel, and M. Kunt. Performance comparison of masking models based on a new psychovisual test method with natural scenery stimuli. *Signal Processing: Image Communication*, 17(10):807 – 823, 2002. ISSN 0923-5965.
- [22] G. Cao, M. Pedersen, and Z. Barańczuk. Saliency models as gamut-mapping artifact detectors. In *5th European Conference on Colour in Graphics, Imaging, and Vision (CGIV)*, pages 437–443, Joensuu, Finland, Jun 2010. IS&T.
- [23] K. B. Raja and M. Pedersen. Artifact detection in gamut mapped images using saliency. In *The Colour and Visual Computing Symposium 2013*, Gjøvik, Norway, Sep. 2013. Accepted.
- [24] J. Harel, C. Koch, and P. Perona. Graph-based visual saliency. In *Proceedings of Neural Information Processing Systems (NIPS)*, pages 545–552, 2006.
- [25] T. Judd, F. Durand, and A. Torralba. A benchmark of computational models of saliency to predict human fixations. Technical report, Massachusetts institute of technology, 2012. MIT-CSAIL-TR-2012-001.
- [26] E. Peli. Contrast sensitivity function and image discrimination. *Journal of the Optical Society of America A*, 18(2):283–193, 2001.
- [27] Z. Wang and J. Y. Hardeberg. Development of an adaptive bilateral filter for evaluating color image difference. *Journal of Electronic Imaging*, 21(2):023021–1–023021–10, 2012.
- [28] Z. Wang and J. Y. Hardeberg. An adaptive bilateral filter for predicting color image difference. In *Color Imaging Conference*, pages 27–31, Albuquerque, NM, USA, Nov 2009. IS&T/SID.
- [29] R. G. Newcombe. Two-sided confidence intervals for the single proportion: comparison of seven methods. *Statistics in Medicine*, 17(8):857–872, 1998.